Geophysical Research Letters

RESEARCH LETTER
10.1029/2022GL100836

Increasing Precipitation Efficiency Amplifies Climate Sensitivity by Enhancing Tropical Circulation Slowdown and Eastern Pacific Warming Pattern

Ryan L. Li[1], Joshua H. P. Studholme[1], Alexey V. Fedorov[1,2], and Trude Storelvmo[3]

[1]Yale University, New Haven, CT, USA, [2]Sorbonne University, Paris, France, [3]University of Oslo, Oslo, Norway

Abstract The role of precipitation efficiency (PE)—the fraction of column-integrated condensate that reaches the surface as rain—in the global temperature response to CO_2 rise is yet to be quantified. Here we employ 36 limited-domain cloud resolving models (CRMs) from the Radiative-Convective Equilibrium Model Intercomparison Project and find that they strongly imply higher PE at warmer temperatures. We then analyze 35 general circulation models (GCMs) from the Coupled Model Intercomparison Project Phase 6 and find that increasing PE is associated with tropical circulation slowdown and greater eastern equatorial Pacific warming. These changes trigger pan-tropical positive cloud feedback through stratiform anvil cloud reduction and stratocumulus suppression, resulting in higher Effective Climate Sensitivity (ECS). We find that in 24 of 35 GCMs matching the CRMs in simulating increasing PE with greenhouse warming, mean ECS is 1 K higher than in PE-decreasing GCMs. Thus, further constraining PE sensitivity to temperature could reduce uncertainty over future climate projections.

Plain Language Summary Precipitation efficiency (PE) is the ratio of precipitation to cloud condensate. Evidence from the great majority of cloud-resolving models and many earth system models support higher PE with warming. With higher PE, more cloud condensate leaves the atmosphere as precipitation, reducing cloud cover and optical thickness. As PE is tightly linked to the latent heat release of tropical convection, an atmosphere with high PE and a weak circulation can release the same latent heat as its counterpart with low PE and strong circulation. Increasing PE is robustly correlated with pan-tropical positive cloud feedback in the equatorial Pacific, namely thinner stratiform anvil clouds in the west and suppressed stratocumulus cloud cover in the east. Hence, quantifying PE change is critical for climate projections.

Ryan Li and Joshua Studholme share lead authorship.

Key Points:

- Cloud-resolving models indicate increasing precipitation efficiency with global warming
- High precipitation efficiency implies a weak Walker circulation, eastern tropical Pacific warming, and positive tropical cloud feedback
- All 4 K or higher climate sensitivity climate models project increasing precipitation efficiency

Supporting Information:

Supporting Information may be found in the online version of this article.

Correspondence to:

R. L. Li,
ryan.li@yale.edu

Citation:

Li, R. L., Studholme, J. H. P., Fedorov, A. V., & Storelvmo, T. (2023). Increasing precipitation efficiency amplifies climate sensitivity by enhancing tropical circulation slowdown and eastern Pacific warming pattern. *Geophysical Research Letters*, *50*, e2022GL100836. https://doi.org/10.1029/2022GL100836

Received 15 AUG 2022
Accepted 24 DEC 2022

Author Contributions:

Conceptualization: Ryan L. Li, Joshua H. P. Studholme, Alexey V. Fedorov, Trude Storelvmo
Funding acquisition: Alexey V. Fedorov, Trude Storelvmo
Investigation: Ryan L. Li, Joshua H. P. Studholme
Methodology: Ryan L. Li, Joshua H. P. Studholme, Alexey V. Fedorov
Project Administration: Alexey V. Fedorov, Trude Storelvmo

1. Introduction

The atmospheric circulation over the tropical Pacific couples intense turbulent ascent in the west to slow stable descent in the east. Over the western tropical Pacific, horizontally extensive ice clouds, known as anvil clouds, cap deep tropical cumuliform clouds and cover a much larger fraction of the troposphere than their lower-level cloud cores. These optically thick cores are Earth's most reflective clouds and thereby represent a significant negative contributor to the planetary energy budget. Above them, the cold anvil clouds have a correspondingly strong positive contribution to the energy budget by absorption of longwave radiation (Hartmann & Berry, 2017). In the east, shallow stratocumulus clouds mark the vertical boundary between the warm descending air of remote origin and shallow local overturning cells (Wood & Bretherton, 2006). These clouds are highly reflective to incoming shortwave radiation, but due to their low altitude and low cloud top temperatures relative to the surface, they have negligible effects on outgoing longwave radiation. The mechanisms governing these two contrasting cloud types are the dominant sources of uncertainty in assessments of Earth's climate sensitivity (Forster et al., 2021; Sherwood et al., 2020), a "multi-trillion-dollar" research question (Hope, 2015).

The notion of precipitation efficiency (PE) represents the fraction of condensate to fall to the surface as precipitation, the residual condensate being left behind in the form of clouds. Structurally PE is related to the complex microphysical processes that govern the growth of ice crystals and cloud droplets (Stevens & Feingold, 2009) which can reach the surface as precipitation particles. Thermodynamically, PE represents the fractional latent heat release of atmospheric convection. The other fraction of the total condensate re-evaporates, thereby reabsorbing the latent heat released in the original condensation. This links PE to the net energetics of deep convection and thereby to convective updraft strength (K. Emanuel, 2019). The mechanisms which set PE largely depend on the humidity of the atmosphere in regions of precipitation. This follows from droplets falling through humid

Resources: Ryan L. Li, Joshua H. P. Studholme
Software: Ryan L. Li, Joshua H. P. Studholme
Supervision: Alexey V. Fedorov, Trude Storelvmo
Visualization: Joshua H. P. Studholme
Writing – original draft: Ryan L. Li, Joshua H. P. Studholme
Writing – review & editing: Ryan L. Li, Joshua H. P. Studholme, Alexey V. Fedorov, Trude Storelvmo

air evaporating less than when falling through drier air (Houze, 2014). However, PE also depends on droplet size, local air temperature and other factors. For example, although tropical mean relative humidity is expected to be constant under greenhouse warming, recent cloud-resolving model (CRM) studies suggest higher PE in warmer climates due to increasing cloud density (Lutsko & Cronin, 2018) and convective organization (Bao & Sherwood, 2019; Fildier et al., 2021).

While other factors influencing atmospheric convection at a range of scales have been studied extensively, such as sea surface temperatures (SSTs; Emanuel et al., 1994) and free tropospheric humidity (Bretherton et al., 2004; Held & Soden, 2006), the role of PE is poorly understood. This is partly the result of PE being extremely difficult to measure because of the microphysical nature of rain formation, cloud condensation, and evaporation (Lutsko et al., 2021). It is also the result of definitions and representations of PE varying immensely across observational and modeling studies (Sui et al., 2020), making them difficult to synthesize. As a consequence, the role of PE in setting Earth's climate sensitivity is yet to be firmly established. Previous work (Li et al., 2019; Mauritsen & Stevens, 2015; Sherwood et al., 2014; Zhao, 2014) has proposed somewhat conflicting mechanisms through which PE might impact Effective Climate Sensitivity (ECS) but evidence to support these hypotheses is inconsistent across different global climate models (GCMs; see Lutsko et al. (2021) for a review). While simulated cloud responses from imposed PE changes are structurally complex and model dependent, reduction in cloud liquid and ice water path (i.e., the vertically integrated liquid and ice within an atmospheric column) at higher PE is unequivocal (Li et al., 2019; Mauritsen & Stevens, 2015; Zhao, 2014). Reductions in cloud liquid and ice in anvil clouds can contribute to positive cloud feedback due to reduced albedo.

In the present study we quantify PE using a parameter ϵ defined as $\epsilon = P_s/\mathrm{CWP}$, where P_s is surface precipitation and CWP is condensed water path (Methods; Li et al., 2022). PE is often defined as a fraction of unity by normalizing P_s to a measure of condensation rate, such as the ratio of P_s to condensation in the atmospheric column. However, local condensation is difficult to measure and compute, which leads to a wide range of PE estimates from 0.1 to greater than 1.0 (Sui et al., 2020). Vigorous hydrological cycling of the atmosphere requires that condensation constantly replenishes the relatively small stock of CWP, and so variations of condensation rate and CWP are closely related (Li et al., 2022). Thus, the parameter ϵ, which is tightly correlated with microphysical measures of PE, captures microphysical cloud condensation at the macrophysical scale and is indeed a measure of PE (Li et al., 2022). Unlike other existing PE metrics, ϵ enables comparable estimates of PE across observations, CRMs and GCMs. For the remainder of this study, we use ϵ and PE interchangeably, and compute climatological ϵ to represent the net effect of different cloud regimes, from deep convective clouds to non-precipitating shallow clouds, within the tropical cloud ensemble.

The goal of the study is to quantify and explain the effect of PE on the planet's equilibrium temperature response after greenhouse gas increases. Investigating cloud-resolving simulations in the Radiative-Convective Equilibrium Model Intercomparison Project (RCEMIP; Wing et al., 2020), we find that they imply PE should increase with warming. To understand what this means for climate sensitivity, we then analyze ϵ in 35 GCMs participating in Phase 6 of the Coupled Model Intercomparison Project (CMIP6; Eyring et al., 2016). Using these GCMs we identify two key components linking increasing PE with the resultant warming: (a) high cloud feedback associated with retreat and thinning of convective anvils over the western tropical Pacific and (b) low cloud feedback resulting from suppression of stratocumulus decks in the eastern tropical Pacific. These mechanisms are linked via the magnitude of Pacific Walker circulation slowdown, whereby higher PE with greenhouse warming amplifies circulation weakening. The positive feedback mechanisms (a) and (b) act to amplify the overall warming leading to a higher climate sensitivity, while a stronger eastern equatorial Pacific warming pattern mirrors the greater slowdown of the Walker circulation.

2. Materials and Methods

2.1. Precipitation Efficiency Measure

We use the measure of PE:

$$\epsilon = \frac{P_s}{\mathrm{CWP}}, \tag{1}$$

where P_s is the surface precipitation rate and CWP is vertically integrated condensed water and ice in the atmospheric column. ϵ has high correspondence with the microphysical definition of PE (Li et al., 2022). ϵ is computed

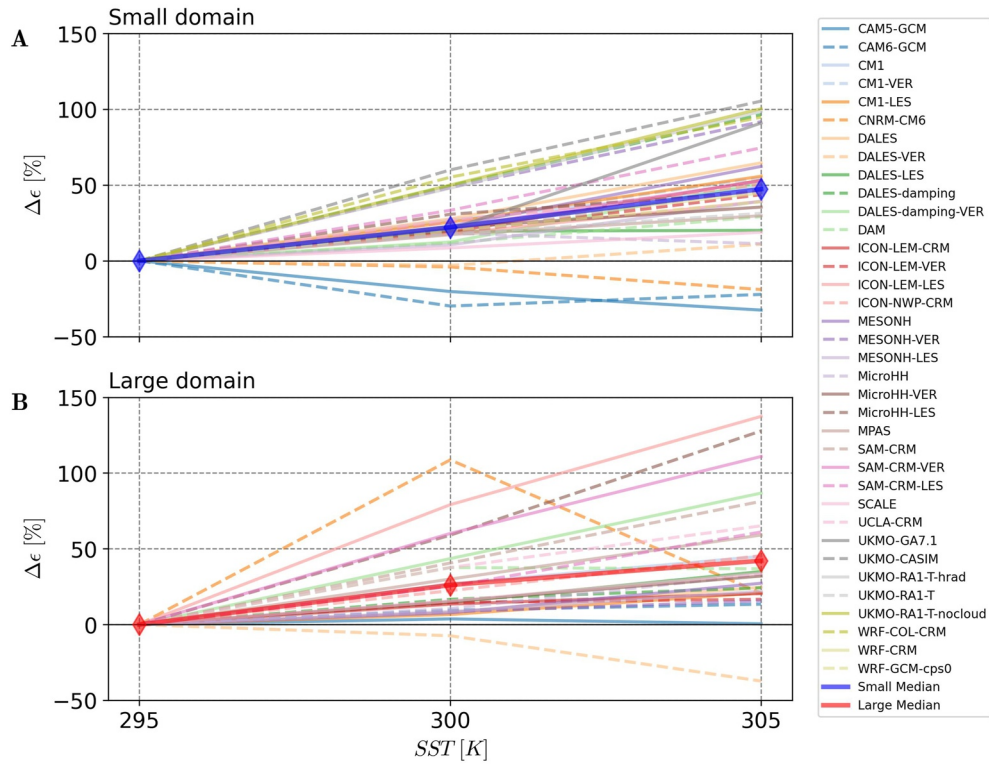

Figure 1. High-resolution model ensemble indicate positive ϵ sensitivity. Change in precipitation efficiency $\Delta\epsilon$ versus Sea Surface Temperature (SST) simulated in (a) small and (b) large domains by large-eddy simulations, cloud-resolving models, single-column models, and general circulation models participating in the RCEMIP. Units are indicated in square brackets. Among the 36 small and 28 large domain experiments available, 32 small domain models and 26 large domain models show increasing PE with warming. Change is relative to the 295 K simulation. Diamonds show median ϵ sensitivity across all models.

at each grid and then averaged, with the exception of CRM data where P_s and CWP are averaged over the whole domain prior to calculating their ratio. PE's inverse $\epsilon^{-1} = \tau_c$ is a characteristic residence timescale for the total condensed cloud water across an ensemble of cloud types. τ_c is a characteristic drying timescale for the atmosphere if condensation has stopped, where high ϵ is equivalent to low τ_c signaling shorter residence time of clouds and high precipitation efficiency. The exclusive use of macrophysical variables enables consistent ϵ data in CRMs, GCMs and observations.

In GCMs, changes in ϵ with surface temperature increase is determined by the representation of deep convection within the models, namely whether convective rainout is a function of vertical mass flux (Li et al., 2022). While models with positive ϵ sensitivity to temperature generally show decreases in CWP and higher fractional increases in P_s, the difference in ϵ sensitivity cannot be explained by P_s nor CWP alone. Rather, differences in the greenhouse warming response of ϵ encapsulates a wide range of P_s and CWP perturbations (Figure 1a and Figure S1 in Supporting Information S1). The origin of different GCM behavior is due to differences in the convective precipitation formulation.

2.2. Cloud Resolving Model Estimates of ϵ

We use results from the CRM experiments in the RCEMIP, which are run on a doubly-periodic domain with perpetual sunlight, fixed and uniform SSTs, and no rotation (Wing et al., 2020). Small domain simulations use a square domain of 100 km by 100 km and a horizontal resolution of 1 km. Large domain simulations employ a channel geometry of 400 km by 6,000 km with 3 km horizontal resolution, allowing the possibility of convective organization. To compute ϵ, we use domain-averaged diagnostics of precipitation and condensed water path for small and large domain simulations at 295, 300, and 305 K SSTs provided by Dr. Allison Wing. Fractional change in ϵ, $\Delta\epsilon/\epsilon$, for each model is computed relative to the 295 K SST simulation.

2.3. CMIP6 Data

Thirty-five models from CMIP6 are used in this study to compute ϵ, all models with available output in the CMIP6 data repository in both the preindustrial control (piControl) and abrupt quadrupling of atmospheric CO_2 (abrupt-4xCO_2) scenarios. Environmental metrics and sensitivity of ϵ to greenhouse warming is defined as the change in ϵ spatially averaged from 30°S to 30°N and monthly data temporally averaged over the final 50 years in abrupt-4xCO_2 relative to piControl.

2.3.1. Models With Negative ϵ Sensitivity (Total 11)

AWI-CM-1-1-MR, CAMS-CSM1-0, FGOALS-g3, GFDL-CM4, GFDL-ESM4, GISS-E2-1-G, GISS-E2-1-H, GISS-E2-2-G, MPI-ESM-1-2-HAM, MPI-ESM1-2-HR, and MPI-ESM1-2-LR.

2.3.2. Models With Positive ϵ Sensitivity (Total 24)

BCC-CSM2-MR, BCC-ESM1, CESM2, CESM2-FV2, CESM2-WACCM, CESM2-WACCM-FV2, CIESM, CMCC-CM2-SR5, CMCC-ESM2, CanESM5, E3SM-1-0, EC-Earth3-AerChem, IITM-ESM, INM-CM4-8, INM-CM5-0, IPSL-CM5A2-INCA, IPSL-CM6A-LR, KACE-1-0-G, MIROC6, MRI-ESM2-0, NorESM2-LM, NorESM2-MM, SAM0-UNICON, and TaiESM.

3. Results

3.1. Sensitivity of ϵ to Temperature in Convection-Permitting CRMs

We begin by considering PE's relationship with surface temperature in 36 models participating in the RCEMIP. These experiments are separated into two domain sizes: "small" defined as 100×100 km^2 and "large" defined as $400 \times 6{,}000$ km^2. Convective self-aggregation is for the most part absent in the small domain simulations but is present in the large domains. The great majority of RCEMIP models predict increasing PE with warming (Figure 1): 32 out of 36 models in the small domain experiments and 26 out of 28 models in the large domain experiments. The median estimates for ϵ sensitivity, 4.5 %K^{-1} in small domains and 3.3 %K^{-1} in large domains, agree with estimates from positive ϵ sensitivity GCMs under gradual greenhouse forcing which range from 1 to 5 %K^{-1} (Li et al., 2022). These findings bolster previous single model results that indicated PE will increase with warming (Bao & Sherwood, 2019; Lutsko & Cronin, 2018).

3.2. Link Between ϵ and Tropical Cloud Feedback in CMIP6

Since cloud-resolving models imply PE increases with warming, we then investigate the significance of this change for large-scale climate. To do this we separate CMIP6 GCMs into two groups based on the sign of the models' tropical-mean ϵ change following increased atmospheric CO2 concentrations (Materials and Methods). These ϵ changes, defined at each grid, are subsequently referred to as ϵ sensitivity. Applying this separation criterion cleanly divides CMIP6 models into two sets (Figure 2a). Dividing these models on either the precipitation sensitivity or CWP sensitivity alone does not yield two distinct groups of models. This clean PE separation was traced to the GCMs' choice of convection parameterization (Li et al., 2022).

Spatial differences in ϵ changes between the two model groups are prominent throughout the tropics and in heavy precipitation regions (Figures 2b and 2c). The sign of models' overall ϵ sensitivity matches up with the sign of the ϵ change in the Indo-Pacific warm pool (WP; defined as the overlain box in Figure 2b between 20°S–20°N and 80°E–180°E). In the equatorial Eastern Pacific (EP; 30°S–30°N and 80°W–180°W), ϵ increases in both model groups but in models with positive ϵ sensitivity this ϵ increase is twofold greater than in models with negative ϵ sensitivity.

We find that ϵ sensitivity is proportional to the local net cloud feedback in both the WP and EP ($r = 0.60$ and 0.51 respectively; Figure 2d). In positive ϵ sensitivity models, the net WP cloud feedback is dominated by the shortwave component and only partially compensated in the longwave (Figure S2 in Supporting Information S1), resulting in a net positive cloud feedback compared to negative ϵ sensitivity models. The dominance of the shortwave feedback in this group of GCMs means that the sign of the overall WP cloud feedback opposes the sign expected by the proposed infrared iris effect (Mauritsen & Stevens, 2015). This is in agreement with results of other GCM sensitivity studies that imposed higher convective rainout and consequently higher PE (Li et al., 2019; Zhao, 2014). This PE–cloud feedback relationship suggests a mechanism whereby enhanced convective rainout limits detrainment and the reduced anvil cloud source results in their contraction and thinning.

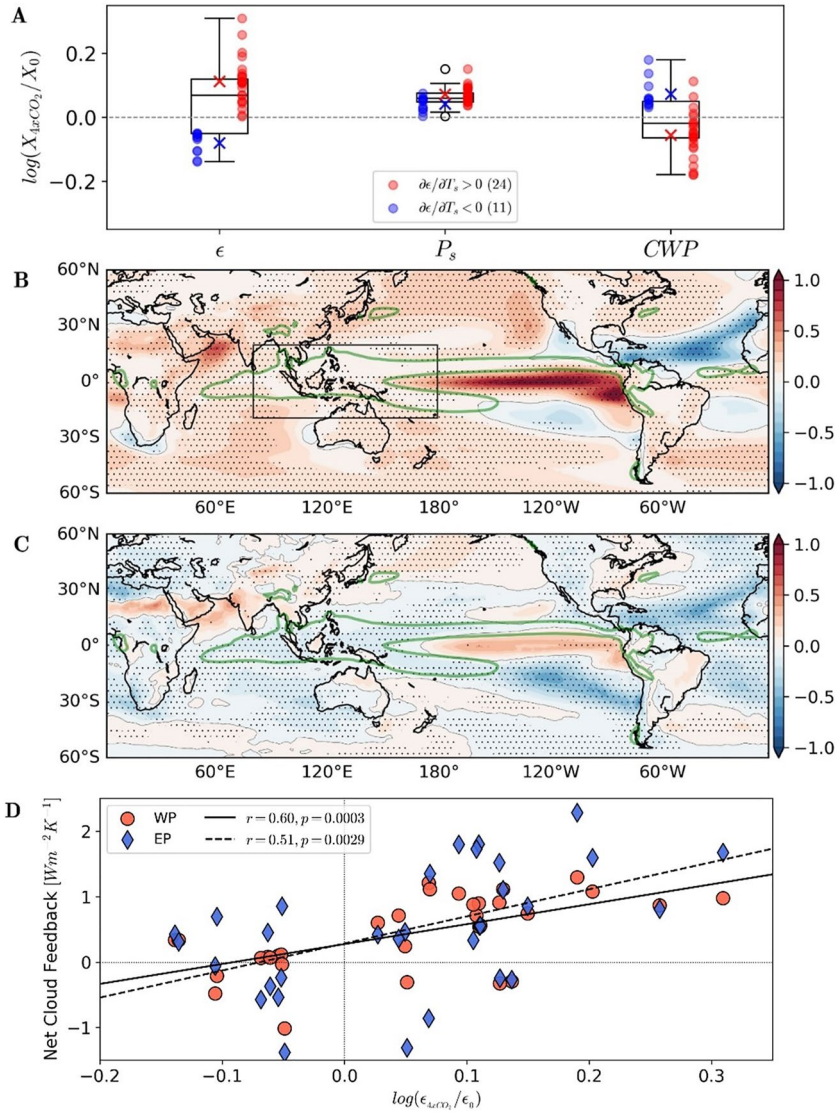

Figure 2. Impact of the disagreement of precipitation efficiency sensitivity in CMIP6. (a) Sensitivity of tropical ϵ, precipitation (P_s), and condensed water path (CWP) to greenhouse warming for two groups of climate models: with positive (red) and with negative (blue) sensitivities of tropical-mean (30°S–30°N) ϵ to greenhouse warming. (b, c) Spatial maps of multi-model mean ϵ sensitivity for models with positive and with negative ϵ sensitivities, respectively. Stippling in (b, c) indicates more than 75% of models agree on the sign of the response. Green contours outline regions with 6 mm per day or more surface precipitation in the annual mean. (d) Net cloud feedback estimated over the Indo-Pacific Warm Pool (WP; black box in panel b; circles) and over the Eastern Pacific (EP; diamonds) scattered against tropical ϵ sensitivity to greenhouse warming for different models. The solid and dashed lines represent linear regressions for WP and EP data, respectively, where r is the Pearson correlation coefficient and p is the associated p value. Overall, higher values of cloud feedback correspond to positive ϵ sensitivity. See Methods for CMIP6 model and simulation details.

The similar correlation magnitudes between ϵ sensitivity and net cloud feedback in both the WP and EP hint at a mechanistic link coupling the cloud feedbacks across the entire Pacific (Figure S4 in Supporting Information S1). The net cloud feedback difference over the EP between GCMs with positive versus negative ϵ sensitivity is also dominated by the shortwave component (1.18 W m^{-2} K^{-1}, Figure S2 in Supporting Information S1). Additionally, this is slightly offset by a longwave component (– 0.36 W m^{-2} K^{-1}), and sums to a net value of 0.82 W m^{-2} K^{-1}.

Consequently, CMIP6 models with positive ϵ sensitivity exhibit stronger positive cloud feedbacks in both the WP and EP relative to their counterparts with negative ϵ sensitivity (Figure S2 in Supporting Information S1). In the average over the entire tropics, the net cloud feedback difference between the two model groups is 0.49 W m^{-2} K^{-1}

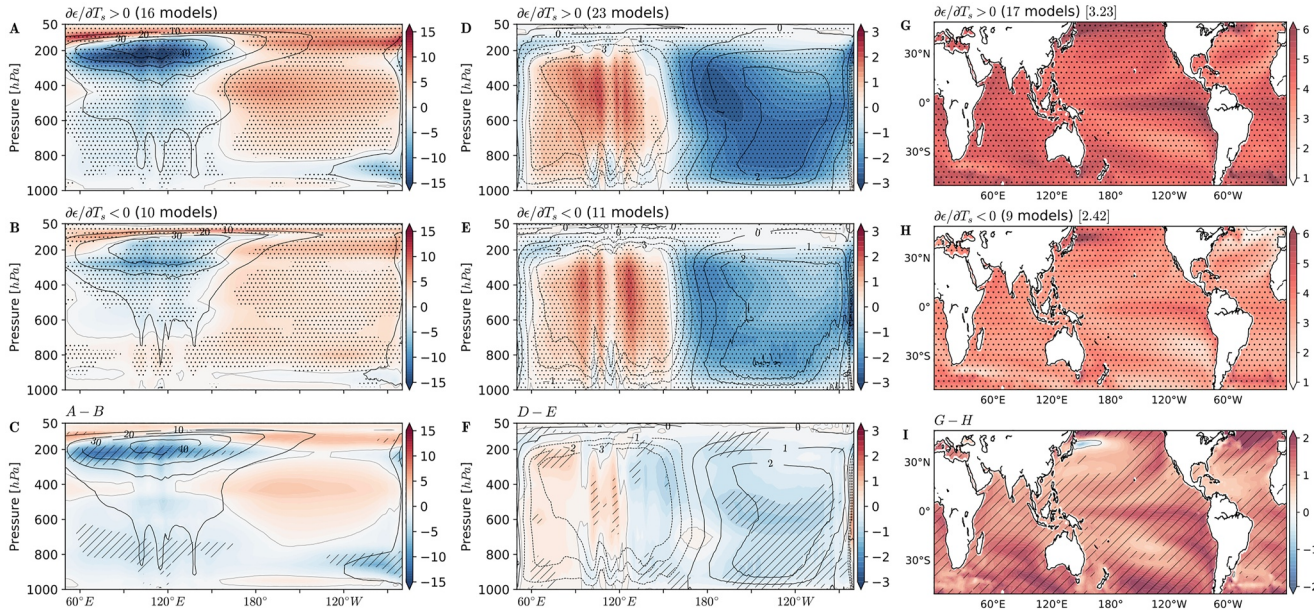

Figure 3. Contraction and thinning of deep convective anvil clouds, low stratocumulus cloud suppression, Walker circulation weakening, and enhanced Eastern Pacific warming. Changes in cloud areal coverage (cloud fraction) along the equator in response to greenhouse warming in (a) positive and (b) negative ϵ sensitivity models, and (c) the difference between the two, that is, panel (a) minus panel (b). (d–f) As the left column but for changes in vertical pressure velocity. (g–i) As the left column but for changes in sea surface temperature. Black contours in (a–f) show multi-model mean preindustrial climatology. In the titles of panels, square brackets indicate the tropical mean SST (30°S–30°N) and round brackets indicate the number of models. Stippling indicates more than 75% of models agree on the sign of the response; hatching shows p-value less than 0.05 using Welch's *t*-test. Cloud fraction is given in % spatial coverage, velocity in 10^{-2} Pa per second, and SST in K. Experiments with abrupt quadrupling of atmospheric CO_2 relative to preindustrial control have been used. For the left and middle columns, the data is averaged between 5°S–5°N.

(Figure S2a in Supporting Information S1). This net feedback is the sum of larger positive shortwave feedback $\left(0.89\mathrm{W m^{-2}\,K^{-1}}\right.$, Figure S2b in Supporting Information S1) being partly compensated by smaller negative longwave feedback $\left(-0.40\mathrm{W\,m^{-2}\,K^{-1}}\right.$, Figure S2c in Supporting Information S1). A decomposition analysis by cloud height (Methods) reveals the dominant contributions come from medium and high clouds in the WP and low clouds in the EP (Figure S3 in Supporting Information S1). The WP medium and high net cloud feedback of $0.40\,\mathrm{W\,m^{-2}\,K^{-1}}$ (Figure S3a in Supporting Information S1) and the EP low cloud net feedback of $0.51\,\mathrm{W\,m^{-2}\,K^{-1}}$ (Figure S3d in Supporting Information S1) are tightly linked (correlation coefficient $r = 0.64$, Figure S4 in Supporting Information S1).

3.3. Walker Circulation Slowdown, Anvil Cloud Reduction and Stratocumulus Suppression

We connect this array of cloud feedback differences across the Pacific to the concomitant enhanced slowdown of the Walker circulation in positive versus negative ϵ sensitivity GCMs (Figure 3). The differences in the large-scale circulation slowdown are statistically significant in the ascending WP and subsiding EP (Figure 3f). In the convectively active WP, anvil cloud fraction reduces as the planet warms and the large-scale circulation slows (Figures 3a and 3b), a feature of both groups of GCM simulations. The reduction of cloud cover peaks near the climatological anvil cloud maximum at 120°E and 200 hPa, where there is a strong difference in the magnitude of this effect between positive (15%) and negative (5%) ϵ sensitivity models (Figure 3c). From the top of the atmosphere, these simulated changes appear as a contraction in the area covered by anvil clouds as well as thinning (Figure S5 in Supporting Information S1) since the clouds are less opaque to sunlight. In the EP, the radiatively bright stratocumulus clouds are capped from above by the descending branch of the Walker circulation. In our results, associated with the enhanced large-scale circulation slowdown in positive ϵ sensitivity models, these EP stratocumulus decks are suppressed (Figure 3c). This triggers a very strong local shortwave cloud feedback (Figure S3c in Supporting Information S1). We think this is very likely the dominant cause of the enhanced southern hemisphere Eastern Pacific SST warming (Figure 3i).

The Walker circulation weakening being effectively controlled by PE change can be qualitatively interpreted by first considering the energetic constraint on vertical mass flux in the tropical atmosphere. In Held and

Soden (2006), their original constraint $P = Mq$, where P is surface precipitation, M is the mass flux exchange between the boundary layer and free troposphere, and q is specific humidity. Taking the differential leads to

$$\frac{dM}{M} = \frac{dP}{P} - \frac{dq}{q}, \tag{2}$$

where changes in the mass flux are constrained by changes in precipitation and specific humidity. Per degree K of warming, specific humidity increases by about 7%, following the Clausius-Clapeyron relation, while precipitation increases by roughly 2%, constrained by infrared radiation increase. This implies that the vertical mass flux should decrease by about 5%. The Walker circulation slowdown with global warming is qualitatively consistent with this argument, though actual numbers may differ depending on the metric. Now adding PE to this relation yields $P = \epsilon_m Mq$, where ϵ_m is the dimensionless microphysical PE (i.e., surface precipitation over vertically integrated condensation rate; Lutsko & Cronin, 2018; Sui et al., 2020). Taking the differential again yields

$$\frac{dM}{M} = \frac{dP}{P} - \frac{dq}{q} - \frac{d\epsilon_m}{\epsilon_m}, \tag{3}$$

where changes in PE also contribute to changes in the vertical mass flux. If PE decreases with global warming, the vertical mass flux can decrease less. If PE increases, the mass flux has to decrease more, which implies an enhanced weakening of the Walker circulation.

With enhanced Walker circulation slowdown by increasing PE, the equatorial surface easterlies are correspondingly weakened (Figure S6 in Supporting Information S1). It thus follows that this reduced wind stress dampens the climatological oceanic upwelling at the equator and off South America's western coast. This second order effect of increasing PE is evident in an El Nino-like SST warming pattern (Figure 3i). This adds to the Eastern Pacific warming caused by the local stratocumulus suppression. In addition to these two effects, warmer SSTs and weaker surface temperature inversion (Figure S7 in Supporting Information S1) create less favorable conditions for stratocumulus decks (Wood & Bretherton, 2006). Amplification of these effects in positive ϵ sensitivity GCMs further contributes to the reduction of low clouds and thus establishes the positive cloud feedback in the EP (Figure S3e in Supporting Information S1).

Tropical ϵ is associated with shallow and deep convection. Given that climatological deep convection in the WP is strongest, one might hypothesize that it is the driver of PE's influence. However, WP anvil clouds have cold cloud tops, and reduced fractional cover accompany local negative longwave feedback (Figure S3c in Supporting Information S1). This partly compensates the positive shortwave feedback (Figure S3b in Supporting Information S1) and thus dampens the net anvil cloud feedback (Figure S3a in Supporting Information S1). On the other hand, PE changes on annual and longer decadal time scales are also strong in positive ϵ sensitivity models in the low cloud dominant EP (Figure 2b). This could be explained by changes in transient deep convection in the EP or more strongly precipitating shallow convection. PE's influence is pan-tropical and profoundly coupled to the clouds and convective circulation.

The Walker circulation connects a diverse array of tropical cloud regimes. In the WP, positive anvil cloud feedback amplifies the local warming, which is enhanced at higher altitudes by moist adiabatic adjustment (Figure S8 in Supporting Information S1). As the weak effective planetary rotation cannot sustain horizontal temperature gradients (Sobel et al., 2001), PE induced changes in the WP is communicated throughout the tropics. With higher PE, measured by increased ϵ, updrafts become more efficient, wherein a weaker circulation sustains the same latent heating (Figures 3d–3f). The Walker circulation bridges the WP and EP cloud feedback, and, under greenhouse warming, increasing ϵ causes greater Walker circulation slowdown, amplifying the positive cloud feedback.

3.4. PE's Link to Climate Sensitivity

Collectively these results reveal that the integrated links between enhanced large-scale circulation slowdown and the cloud changes across the Pacific associated with PE changes result in an overall positive cloud feedback. This suggests that PE amplifies warming following increases in greenhouse gases. We quantify this effect by considering these models ECS values and find that positive ϵ sensitivity is a necessary but insufficient condition for high ECS (Figure 4a). In the 24 out of the total 35 CMIP6 GCMs which match the cloud-resolving models

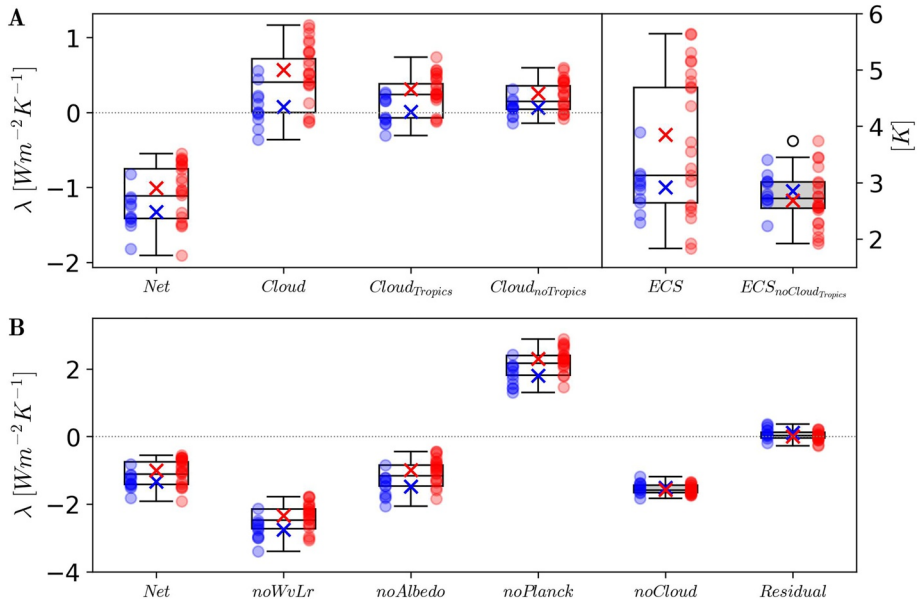

Figure 4. Role of tropical cloud feedback in ECS spread. (a) The Net feedback (sum of all individual climate feedbacks) and Cloud feedback for 35 GCMs employed in this study. The Cloud feedback is decomposed into contributions from tropical clouds (30°S–30°N; $Cloud_{Tropics}$) and extratropical clouds (90–30°S and 30–90°N; $Cloud_{Extratropics}$). Effective Climate Sensitivity (ECS) is defined as the effective radiative forcing of CO2 doubling divided by the net climate feedback parameter (Zelinka et al., 2020). The multi-model mean ECS for positive and negative ϵ sensitivity models are 3.84 K and 2.91 K, respectively. A hypothetical ECS estimate that assumes zero tropical cloud feedback ($ECS_{NoCloud_{Tropics}}$) is also provided. (b) The Net feedback with each individual feedback component removed: water vapor and lapse rate (noWvLr), albedo (noAlbedo), Planck (noPlanck), and cloud (noCloud). Without cloud feedback, the feedback parameters are indistinguishable from the residual term in the linear framework. Units are given in square brackets.

in simulating increasing PE with greenhouse warming, mean ECS is 1 K higher than in GCMs in which PE decreases. While models with positive ϵ sensitivity exhibit both high and low ECS estimates, all negative ϵ sensitivity models have low end ECS. Moreover, all GCMs with ECS greater than 4 K (10 of 35 models) have positive ϵ sensitivity (Figure 4a).

We decompose ECS into its individual feedback components to confirm that the above mentioned ECS differences are dominated by tropical clouds. Among all possible feedbacks, only assuming zero cloud feedback results in the two model groups becoming statistically indistinguishable (Figure 4b). Furthermore, the two model groups become statistically indistinguishable in a separate ECS calculation assuming zero tropical cloud feedback (Figure 4a). When tropical clouds are excluded from the ECS calculation, all ECS estimates above 4 K disappear, affirming the critical importance of tropical cloud feedback for very high climate sensitivity. We note here that the relationship is significantly weaker between the magnitude of tropical-mean PE and ECS.

4. Discussion

In this study we use a macrophysical PE measure ϵ, the ratio of surface precipitation to condensed water path, to investigate the climate implications of PE change with global warming. We have shown that the vast majority of CRMs suggest that the PE of deep convective clouds will increase under anthropogenic climate change. These multi-model RCEMIP results agree with recent single model CRM studies (Bao & Sherwood, 2019; Lutsko & Cronin, 2018). Lutsko and Cronin (2018) found that at higher surface temperatures, denser clouds support higher fractional rainout. Re-evaporation of rain is also reduced at warmer temperatures (Emanuel et al., 2014). Moreover, GCMs predict that changes in the large-scale tropical circulation pattern with warming will increase rainfall unevenness (Zhang & Fueglistaler, 2019), that is, there is more convective organization. Further, satellite records, albeit short, show tentative signs that these anticipated changes in ϵ are already appearing (Figure S9 in Supporting Information S1). This may be the result of increases in the frequency of organized deep convection in the 21st century as recently identified in satellite observations (Holloway et al., 2017; Tan et al., 2015).

The amplified Walker circulation slowdown in models with increasing PE is coupled to the development of a stronger eastern equatorial Pacific warming pattern (Figures 3g–3i). This pronounced El Niño-like mean pattern, extending from the eastern Pacific to the dateline along the equator (DiNezio et al., 2009; Xie et al., 2010), is projected to emerge with future warming but its strength varies greatly across the models (Heede & Fedorov, 2021). Thus, the PE considerations provide a potential constraint on the strength of this pattern in the future.

Projecting the radiative effects of Earth's deep convective anvils in different climates has been a major challenge. It remains unclear why the net radiative effect of anvils is near neutral in the present day because these clouds are strongly influenced by processes that remain unresolved in contemporary models (Wall et al., 2019). Nevertheless, in a warmer climate, high clouds remain near the same temperature and thus rise in altitude (Norris et al., 2016). As the clouds rise, temperature stratification increases, and this may result in less mass divergence from convective updrafts. This thermodynamic effect has been hypothesized to reduce tropical high cloud cover (Bony et al., 2016). While we have verified that this effect is indeed present in the CMIP6 models, we find that it is independent from the PE–climate sensitivity mechanism identified in this work (Figure S10 in Supporting Information S1).

While the present analysis focuses on the role of PE and deep convection in circulation weakening and cloud feedback, shallow convection plays a major role in regulating humidity and precipitation in the eastern Pacific (Nuijens et al., 2009). The PE increase realized in both model groups (Figures 2a and 2b) is an avenue for future work. Interestingly, we find that PE change is proportional to mean PE in CMIP6 models (Figure S11 in Supporting Information S1).

Convective clouds becoming more efficient at precipitating is coupled to Walker circulation slowdown in a warmer atmosphere. Simultaneously, powerful positive cloud feedbacks proportional to the PE increase emerge in the western and eastern Pacific. In the Indo-Pacific warm pool, there is contraction and thinning of high clouds. Simultaneously, reduced subsidence triggers stratocumulus suppression which warms underlying SSTs, further weakening stratocumulus decks. The dampened equatorial wind stress associated with enhanced Walker circulation slowdown reduces oceanic upwelling in the EP, which further adds to SST increases and thus the local stratocumulus suppression. Coupling between the Walker circulation slowdown and SST enhances the eastern equatorial Pacific warming pattern. Together, the coupled tropical Pacific cloud feedbacks are positive, causing high climate sensitivity (ECS > 4 K) in state-of-the-art GCMs. Thus, we have shown that changes in the precipitation efficiency of deep convective clouds controls tropical cloud feedback via the rates of tropical circulation slowdown and are important for constraining both global levels and spatial patterns of climate change.

Acknowledgments
The authors thank Dr. Mark Zelinka (Lawrence Livermore National Laboratory) for graciously providing us the decomposed cloud feedbacks and making CMIP6 ECS data publicly available. We also thank Dr. Allison Wing (Florida State University) for kindly providing us the domain-averaged diagnostics of precipitation and condensed water path from the RCEMIP archive. We thank the German Climate Computing Center (DKRZ) for hosting the standardized RCEMIP data. We thank Dr. Nicholas Lutsko (Scripps Institution for Oceanography), Dr. Shineng Hu (Duke University), and Dr. Ivy Tan (McGill University) for helpful discussions of this project. J. H. P. S. and A. V. F. were funded by National Oceanic and Atmospheric Administration under Grant NA20OAR4310377. T. S. was funded by EU H2020 under Grants 758005 and 821205. R. L. L. was funded by National Science Foundation under Grant 1352417. Additional funding to A. V. F. was provided by the ARCHANGE project (ANR-18-MPGA-0001, France).

Data Availability Statement

The RCEMIP (Wing et al., 2020) data used in this study is available at https://swiftbrowser.dkrz.de/public/dkrz_70a517a8-039d-4a1b-a30d-841923f8bc7a/RCEMIP/. The CMIP6 data supporting this study are available from https://pcmdi.llnl.gov/CMIP6/. Data from the CRM experiments and satellite-derived observations of ϵ have been made publicly available at https://doi.org/10.5061/dryad.cc2fqz68d. TRMM data are obtained from https://gpm.nasa.gov/missions/trmm and are interpolated from their native 0.25° by 0.25° resolution to 1° by 1° to match that of the MODIS monthly data available at https://atmosphere-imager.gsfc.nasa.gov/products/monthly.

References

Bao, J., & Sherwood, S. C. (2019). The role of convective self-aggregation in extreme instantaneous versus daily precipitation. *Journal of Advances in Modeling Earth Systems*, *11*(1), 19–33. https://doi.org/10.1002/2018MS001503

Bony, S., Stevens, B., Coppin, D., Becker, T., Reeds, K. A., Voigt, A., & Medeiros, B. (2016). Thermodynamic control of anvil cloud amount. *Proceedings of the National Academy of Sciences of the United States of America*, *113*(32), 8827–8932. https://doi.org/10.1073/pnas.1601472113

Bretherton, C. S., Peters, M. E., & Back, L. E. (2004). Relationships between water vapor path and Precipitation over the tropical oceans. *Journal of Climate*, *17*(7), 1517–1528. https://doi.org/10.1175/1520-0442(2004)017<1517:RBWVPA>2.0.CO;2

DiNezio, P. N., Clement, A. C., Vecchi, G. A., Soden, B. J., Kirtman, B. P., & Lee, S. (2009). Climate response of the equatorial Pacific to global warming. *Journal of Climate*, *22*(18), 4873–4892. https://doi.org/10.1175/2009JCLI2982.1

Emanuel, K. (2019). Inferences from simple models of slow, convectively coupled processes. *Journal of the Atmospheric Sciences*, *76*(1), 195–208. https://doi.org/10.1175/JAS-D-18-0090.1

Emanuel, K., Wing, A. A., & Vincent, E. M. (2014). Radiative-convective instability. *Journal of Advances in Modeling Earth Systems*, *6*(1), 75–90. https://doi.org/10.1002/2013MS000270

Emanuel, K. A., David Neelin, J., & Bretherton, C. S. (1994). On large-scale circulations in convecting atmospheres. *Quarterly Journal of the Royal Meteorological Society*, *120*(519), 1111–1143. https://doi.org/10.1002/qj.49712051902

Eyring, V., Bony, S., Meehl, G. A., Senior, C. A., Stevens, B., Stouffer, R. J., & Taylor, K. E. (2016). Overview of the Coupled Model Intercomparison Project Phase 6 (CMIP6) experimental design and organization. *Geoscientific Model Development*, *9*(5), 1937–1958. https://doi.org/10.5194/gmd-9-1937-2016

Fildier, B., Collins, W. D., & Muller, C. (2021). Distortions of the rain distribution with warming, with and without self-aggregation. *Journal of Advances in Modeling Earth Systems*, *13*(2), e2020MS002256. https://doi.org/10.1029/2020MS002256

Forster, P., Storelvmo, T., Armour, K., Collins, W., Dufresne, J.-L., Frame, D., et al. (2021). Chapter 7: The Earth's energy budget, climate feedbacks, and climate sensitivity. In *Climate change 2021: The physical science basis. Contribution of working group I to the sixth assessment report of the intergovernmental panel on climate change*.

Hartmann, D. L., & Berry, S. E. (2017). The balanced radiative effect of tropical anvil clouds. *Journal of Geophysical Research: Atmospheres*, *122*(9), 5003–5020. https://doi.org/10.1002/2017JD026460

Heede, U. K., & Fedorov, A. V. (2021). Eastern equatorial Pacific warming delayed by aerosols and thermostat response to CO_2 increase. *Nature Climate Change*, *11*(8), 696–703. https://doi.org/10.1038/s41558-021-01101-x

Held, I. M., & Soden, B. J. (2006). Robust responses of the hydrological cycle to global warming. *Journal of Climate*, *19*(21), 5686–5699. https://doi.org/10.1175/JCLI3990.1

Holloway, C. E., Wing, A. A., Bony, S., Muller, C., Masunaga, H., L'Ecuyer, T. S., et al. (2017). Observing convective aggregation. *Surveys in Geophysics*, *38*(6), 1199–1236. https://doi.org/10.1007/s10712-017-9419-1

Hope, C. (2015). The $10 trillion value of better information about the transient climate response. *Philosophical Transactions of the Royal Society A*, *373*(2054), 20140429. https://doi.org/10.1098/rsta.2014.0429

Houze, R. A., Jr. (2014). *Cloud dynamics* (p. 496). Academic Press.

Li, R. L., Storelvmo, T., Fedorov, A. V., & Choi, Y.-S. (2019). A positive iris feedback: Insights from climate simulations with temperature-sensitive cloud–rain conversion. *Journal of Climate*, *32*(16), 5305–5324. https://doi.org/10.1175/JCLI-D-18-0845.1

Li, R. L., Studholme, J. H. P., Fedorov, A. V., & Storelvmo, T. (2022). Precipitation efficiency constraint on climate change. *Nature Climate Change*, *12*(7), 642–648. https://doi.org/10.1038/s41558-022-01400-x

Lutsko, N. J., & Cronin, T. W. (2018). Increase in precipitation efficiency with surface warming in radiative-convective equilibrium. *Journal of Advances in Modeling Earth Systems*, *10*(11), 2992–3010. https://doi.org/10.1029/2018MS001482

Lutsko, N. J., Sherwood, S. C., & Zhao, M. (2021). Precipitation efficiency and climate sensitivity. *Geophysical Monograph Series*. https://doi.org/10.1002/essoar.10507822.1

Mauritsen, T., & Stevens, B. (2015). Missing iris effect as a possible cause of muted hydrological change and high climate sensitivity in models. *Nature Geoscience*, *8*(5), 346–351. https://doi.org/10.1038/ngeo2414

Norris, J., Allen, R., Evan, A., Zelinka, M. D., O'Dell, C. W., & Klein, S. A. (2016). Evidence for climate change in the satellite cloud record. *Nature*, *536*(7614), 72–75. https://doi.org/10.1038/nature18273

Nuijens, L., Stevens, B., & Siebesma, A. P. (2009). The environment of precipitating shallow cumulus convection. *Journal of the Atmospheric Sciences*, *66*(7), 1962–1979. https://doi.org/10.1175/2008jas2841.1

Sherwood, S., Bony, S., & Dufresne, J. L. (2014). Spread in model climate sensitivity traced to atmospheric convective mixing. *Nature*, *505*(7481), 37–42. https://doi.org/10.1038/nature12829

Sherwood, S. C., Webb, M. J., Annan, J. D., Armour, K. C., Forster, P. M., Hargreaves, J. C., et al. (2020). An assessment of Earth's climate sensitivity using multiple lines of evidence. *Reviews of Geophysics*, *58*(4), e2019RG000678. https://doi.org/10.1029/2019RG000678

Sobel, A. H., Nilsson, J., & Polvani, L. M. (2001). The weak temperature gradient approximation and balanced tropical moisture waves. *Journal of the Atmospheric Sciences*, *58*(23), 3650–3665. https://doi.org/10.1175/1520-0469(2001)058%3C3650:TWTGAA%3E2.0.CO;2

Stevens, B., & Feingold, G. (2009). Untangling aerosol effects on clouds and precipitation in a buffered system. *Nature*, *461*(7264), 607–613. https://doi.org/10.1038/nature08281

Sui, C.-H., Satoh, M., & Suzuki, K. (2020). Precipitation efficiency and its role in cloud-radiative feedbacks to climate variability. *Journal of the Meteorological Society of Japan*, *98*(2), 261–282. https://doi.org/10.2151/jmsj.2020-024

Tan, J., Jakob, C., Rossow, W., & Tselioudis, G. (2015). Increases in tropical rainfall driven by changes in frequency of organized deep convection. *Nature*, *519*(7544), 451–454. https://doi.org/10.1038/nature14339

Wall, C. J., Hartmann, D. L., & Norris, J. R. (2019). Is the net cloud radiative effect constrained to be uniform over the tropical warm pools? *Geophysical Research Letters*, *46*(21), 12495–12503. https://doi.org/10.1029/2019GL083642

Wing, A. A., Stauffer, C. L., Becker, T., Reed, K. A., Ahn, M.-S., Arnold, N. P., et al. (2020). Clouds and convective self-aggregation in a multi-model ensemble of radiative-convective equilibrium simulations. *Journal of Advances in Modeling Earth Systems*, *12*(9), e2020MS002138. https://doi.org/10.1029/2020MS002138

Wood, R., & Bretherton, C. S. (2006). On the relationship between stratiform low cloud cover and lower-tropospheric stability. *Journal of Climate*, *19*(24), 6425–6432. https://doi.org/10.1175/JCLI3988.1

Xie, S., Deser, C., Vecchi, G. A., Ma, J., Teng, H., & Wittenberg, A. T. (2010). Global warming pattern formation: Sea surface temperature and rainfall. *Journal of Climate*, *23*(4), 966–986. https://doi.org/10.1175/2009JCLI3329.1

Zelinka, M. D., Myers, T. A., McCoy, D. T., Po-Chedley, S., Caldwell, P. M., Ceppi, P., et al. (2020). Causes of higher climate sensitivity in CMIP6 models. *Geophysical Research Letters*, *47*(1), e2019GL085782. https://doi.org/10.1029/2019GL085782

Zhang, Y., & Fueglistaler, S. (2019). Mechanism for increasing tropical rainfall unevenness with global warming. *Geophysical Research Letters*, *46*(24), 14836–14843. https://doi.org/10.1029/2019GL086058

Zhao, M. (2014). An investigation of the connections among convection, clouds, and climate sensitivity in a global climate model. *Journal of Climate*, *27*(5), 1845–1862. https://doi.org/10.1175/JCLI-D-13-00145.1